Strange Particle Production in Ultra-Relativistic Heavy Ion Collisions at CERN

David Evans

The University of Birmingham
Birmingham B15 2TT
U.K.
e-mail: de@hep.ph.bham.ac.uk

Abstract

Strange particle production is expected to be a useful probe into the dynamics of the hot, dense matter produced in an ultra-relativistic heavy ion collision. In particular, if the hadronic matter undergoes a phase transition into a Quark-Gluon Plasma strange particle production is expected to be increased. In this paper some of the important results from CERN on strangeness production in sulphur-nucleus collisions at 200 GeV/c per nucleon and lead-lead collisions at 160 GeV/c per nucleon are reviewed.

1 Introduction

One of the most interesting predictions of QCD is the possibility that hadronic matter, under extreme conditions of density and temperature, may no longer exist in the familiar hadron phase of baryons and mesons but undergo a phase transition into an asymptotically free gas of quarks and gluons. Such a phase of matter is known as a Quark-Gluon Plasma (QGP). It is believed that the high energy densities produced in a central, ultra-relativistic nucleus-nucleus collisions may be high enough for such a phase transition to take place. A programme of heavy ion collisions started at CERN with the provision of an oxygen beam in 1986 and was followed up the next year with a sulphur beam at 200 GeV/c per nucleon. The sulphur beam was upgraded to a truly heavy ion beam of lead at 160 GeV/c per nucleon in 1994.

If a QGP is formed in the collision, an enhancement of strange particle production is expected[1]. In a QGP there will be copious amounts of gluons[2] giving rise to quark-antiquark production from gluon-gluon interactions. As the mass of strange quarks in a QGP ($\sim$ 150 MeV) is less than the expected temperature of the QGP ($\sim$ 200 MeV) the production of strange quark-antiquark pairs will not be greatly inhibited by their mass. Furthermore, in the baryon-rich system produced in a heavy ion collision the initial abundances of u and d quarks, originating from the nucleons in the colliding ions, are high. The production of further u and d quarks, produced as $u\overline{u}$ and $d\overline{d}$ pairs by gluon-gluon fusion, will therefore be intially suppressed by Pauli Blocking. The production of u, d, and s quarks and antiquarks should reach equilibrium in a few fm/c[2]. The strangeness content in the QGP should then lead to a large production of strange and multistrange particles after hadronisation.

An enhancement of strange particle production could also be produced in a dense hadronic system, a Hadron Gas (HG), given enough time[3]. The time needed for a HG to reach strangeness equilibrium is thought to be more than ten times that needed in a QGP[4] with strange antihyperons and multistrange particles and antiparticles taking longer to reach equilibrium than light particles.

In this review I shall present some of the more important results on strangeness production which came from the CERN experiments using a sulphur beam at 200 GeV/c per nucleon and then summarise the first results to emerge from the new experiments using a lead beam at 160 GeV/c per nucleon. This paper is organised as follows: Section 2 discusses ϕ production, section 3 shows some of the results on multiplicity distributions and strangeness enhancement, section 4 shows results on transverse mass, m_{T} distributions, and section 5 presents results on relative particle yields and multistrange hyperon production. The results from sulphur-nucleus collisions will be summarised in section 6. Results from lead-lead collisions from experiments NA44, NA49, and WA97 are presented in section 7 and the overall summary and conclusions in section 8.

2 ϕ Production

ϕ production has been measured in p-U, O-U, and S-U interactions by the NA38 Collaboration and in p-W and S-W interactions by the HELIOS/3 experiment. In both cases the ϕ is detected through its decay into two muons, $\phi \to \mu^+\mu^-$. Figure 1a shows the fitted $\mu^+\mu^-$ effective mass spectrum from NA38 for $E_{\mathrm{T}} < 42$ GeV. It was observed that the ratio $\phi/(\rho+\omega)$ increased

Figure 1: (a) The fitted $\mu^+\mu^-$ mass spectrum for $E_{\mathrm{T}} < 42$ GeV and (b) the ratio $\phi/(\rho+\omega)$ as a function of the energy density for S-U and O-U interactions normalised to p-U.

with transverse energy, E_{T} in both O-U and S-U interactions and that this ratio was smaller in p-U interactions[5]. Figure 1b shows the ratio $\phi/(\rho+\omega)$ versus E_{T} for p-U, O-U, and S-U interactions.

This result could be due to an increase in ϕ production or a decrease in ρ and ω production in oxygen and sulphur interactions. The ϕ and $\rho+\omega$ were, therefore, normalised to the $\mu^+\mu^-$ continuum between the vector meson and J/ψ mass regions, $1.7 < M(\mu^+\mu^-) < 2.7$ GeV. Figure 2 shows the ϕ/C and $(\rho+\omega)/C$ ratios as a function of transverse energy where the ratios have been normalised to that found in p-U interactions and C denotes the $\mu^+\mu^-$ continuum. The ratio ϕ/C can be seen to increase with $E_{\mathrm{T}}A^{-2/3}$ and is above that seen in p-U interactions while the ratio $(\rho+\omega)/C$ is constant with $E_{\mathrm{T}}A^{-2/3}$ and equal to that seen in p-U interactions.

Since these results were first reported both NA38[6] and HELIOS/3[7] have found an excess of dimuons in this mass interval in S-U and S-W interactions respectively and thus some care needs to be taken when interpreting

Figure 2: (a) ϕ/C and (b) $(\rho+\omega)/C$ as a function of the energy density for O-U and S-U interactions normalised to p-U.

these results. As well as dimuon triggers the HELIOS/3 collaboration took events with no muon requirement but with the same multiplicity thresholds. The number of charged particles from these events was used to normalise their ϕ and $(\rho+\omega)$ samples. Table 1 shows the dependence, on the number of projectile participants, of the ratios $\phi/charged$, $(\rho+\omega)/charged$, and $\phi/(\rho+\omega)$ in S-W interactions together with the corresponding ratios in p-W interactionsi[8]. The ratio $\phi/(\rho+\omega)$ increases when going from p-W to central S-W interactions. Going from p-W to S-W interactions $(\rho+\omega)/charged$ remains constant while $\phi/charged$ increases.

Table 1: Centrality dependence of vector mesons from HELIOS/3

proj. part.	$10^6\phi/charged$	$10^6(\rho+\omega)/charged$	$\phi/(\rho+\omega)$
1 (protons)	0.99 ± 0.06	6.83 ± 0.12	0.138 ± 0.008
3.7 ± 2.9 (rms)	0.80 ± 1.40	7.00 ± 4.00	0.100 ± 0.200
14.5 ± 5.6 (rms)	1.80 ± 0.70	8.50 ± 2.50	0.220 ± 0.080
22.7 ± 5.5 (rms)	1.83 ± 0.55	6.50 ± 0.28	0.254 ± 0.022
26.6 ± 4.8 (rms)	1.56 ± 0.24	8.06 ± 0.64	0.222 ± 0.031
29.4 ± 2.6 (rms)	1.98 ± 0.19	6.89 ± 0.47	0.320 ± 0.031
30.6 ± 1.7 (rms)	2.24 ± 0.27	6.91 ± 0.60	0.321 ± 0.042

To summarise ϕ production, the ratio $\phi/(\rho+\omega)$ increases with centrality and is larger in S-A than in p-A interactions. There may be problems with normalising the ϕ and $(\rho + \omega)$ samples with the dimuon continuum due to a reported excess in dimuon production in S-A interactions. Normalisation with charged particles, however, show an increase in ϕ production when going from p-W to S-W while $(\rho + \omega)$ production remains constant. While an enhancement of ϕ production would be a feature of QGP formation it is not, in itself, evidence and it is possible to account for the observed enhancement without invoking a QGP[9].

3 Multiplicity Distributions

The multiplicity of an event may be interpreted in terms of the number of interacting projectile nucleons *i.e.* the centrality of the collision. The higher the multiplicity, the greater the centrality of the collision and hence the higher the energy density of the resulting fireball. Figure 3 shows an early result

Figure 3: NA35 yields of (a) Λ, (b) K^0, and (c) $\overline{\Lambda}$ divided by the negative multiplicity versus negative multiplicity. White squares correspond to p-S, black circles to S-S, and white circles to p-p interactions.

from the NA35 collaboration which shows strange particle yields, which have been normalised to the number of negative particles produced, as a function of negative particle multiplicity[10]. This figure shows that Λ, K^0, and, $\overline{\Lambda}$ production is increased when going from p-S to central S-S interactions. The enhancement for Λs is about a factor of two. The WA85 collaboration also found that Λ, K^0, and, $\overline{\Lambda}$ production is increased when going from p-W to central S-W interactions[11] by about a factor of two. Figure 4 shows negative particle (h^-), Λ, and $\overline{\Lambda}$ normalised yields from WA85 as a function of the multiplicity measured in their multiplicity microstrips[12]. WA85 do not see

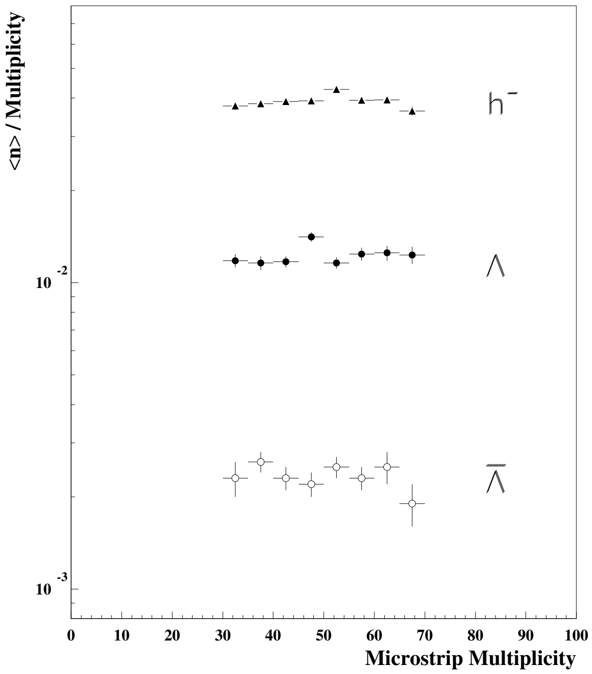

Figure 4: WA85 average number of negatives, Λs, and $\overline{\Lambda}$s divided by microstrip multiplicity as a function of microstrip multiplicity.

any increase of Λ or $\overline{\Lambda}$ production with multiplicity in their multiplicity range. Their trigger, however, is very central. Figure 5 shows the normalised Λ and $\overline{\Lambda}$ yields from NA36 as a function of negative particle multiplicity[13]. The NA36 experiment has a looser trigger than WA85 and so can extend down to lower multiplicities. Figure 5 shows that the hyperon yields increase with respect to negative particle production at low multiplicities before saturating at high multiplicities.

4 Transverse Mass Distributions

The study of transverse mass distributions can yield useful information on the temperature and the degree of flow in the fireball. Data are generally

Figure 5: NA36 Λ and $\overline{\Lambda}$ production divided by the negative multiplicity as a function of the negative multiplcity.

fitted with the expression

$$\left(\frac{1}{m_{\mathrm{T}}}\right)\frac{\mathrm{d}N}{\mathrm{d}m_{\mathrm{T}}} \propto e^{-m_{\mathrm{T}}\beta} \tag{1}$$

or

$$\left(\frac{1}{m_{\mathrm{T}}}\right)^{\frac{3}{2}}\frac{\mathrm{d}N}{\mathrm{d}m_{\mathrm{T}}} \propto e^{-m_{\mathrm{T}}\beta} \tag{2}$$

where $m_{\mathrm{T}} = \sqrt{p_{\mathrm{T}}^2 + m^2}$. Both expressions give similar χ^2s but expression (1) tends to yield a slightly higher inverse slope, β. Table 2 shows the inverse slopes for different particles and reactions from NA35[14, 15] and NA36[16]. The number in the second column indicates whether the data were fitted with expression (1) or expression (2) above.

Table 2: Inverse slopes in MeV from NA35 and NA36.

Reaction		Λ	$\overline{\Lambda}$	K^0	K^+	K^-
NA35 pS	(1)	182 ± 17	132 ± 18	205 ± 16		
	(2)	172 ± 17	126 ± 18	187 ± 16		
NA35 SS	(1)	204 ± 17	180 ± 24	210 ± 16	227 ± 16	270 ± 36
NA35 SAg	(1)	234 ± 17	221 ± 24	231 ± 17	254 ± 31	181 ± 28
	(2)	219 ± 17	209 ± 22	211 ± 16	222 ± 26	163 ± 25
NA35 SAu	(1)	240 ± 18	223 ± 22	227 ± 18		
	(2)	224 ± 18	207 ± 21	208 ± 17		
NA36 pPb	(2)	210 ± 5	177 ± 17	205 ± 11		
NA36 SPb	(2)	207 ± 10	201 ± 10	197 ± 5		

Table 3: Inverse slopes in MeV from WA85 and WA94.

Particle	WA85		WA94	
	p+W	S+W	p+S	S+S
K^+		211 ± 12		172 ± 20
K^-		198 ± 13		152 ± 25
K^0		219 ± 5		
h^-	196 ± 21	235 ± 5		
Λ	197 ± 2	233 ± 3	191 ± 3	213 ± 3
$\overline{\Lambda}$	185 ± 5	232 ± 7	181 ± 5	204 ± 5
Ξ^-	211 ± 14	244 ± 12	212 ± 9	222 ± 10
$\overline{\Xi}^+$	216 ± 21	238 ± 16	202 ± 12	208 ± 13

Table 3 shows the inverse slopes reported from experiments WA85[17, 18, 19] and WA94[20, 21] where all the data have be fitted with expression (2). The first thing to be noted from tables 2 and 3 is that the inverse slopes from proton induced reactions are smaller than the corresponding inverse slopes from sulphur induced reactions in almost all cases. Also, larger targets tend to produce larger inverse slopes. Figure 6 shows the m_{T} spectra for Λ, $\overline{\Lambda}$, Ξ^-, and $\overline{\Xi}^+$ hyperons produced in SW interactions by WA85. It should be noted that in all the WA85 and WA94 results the Λ ($\overline{\Lambda}$) yields have been corrected for *feed-down* from Λs ($\overline{\Lambda}$s) coming from Ξ^- and Ξ^0 ($\overline{\Xi}^+$ and $\overline{\Xi^0}$) decays. In principle this correction should affect all experiments to some degree depending on their geometry, resolution, and selection procedures.

5 Relative Particle Yields

Relative yields for strange hyperons and anti-hyperons have been presented by the NA36[22], WA85[17], and WA94[20] collaborations. The WA85 and

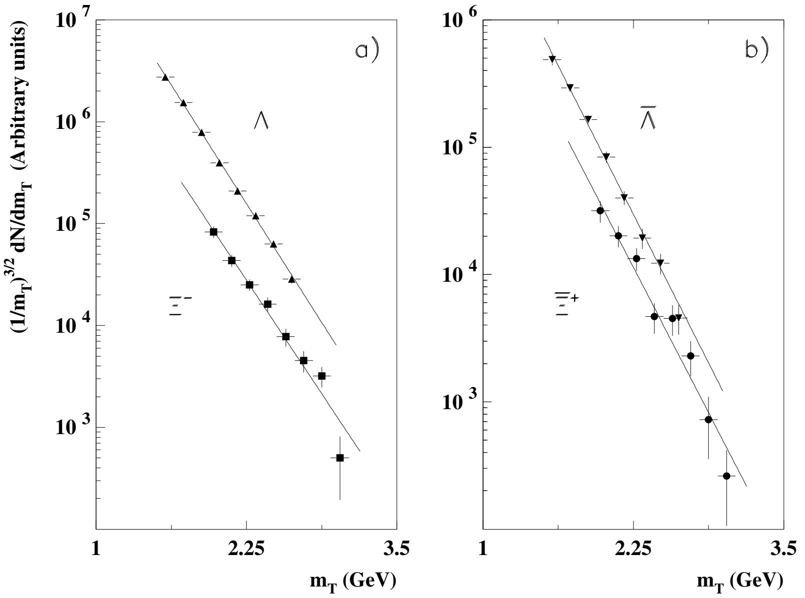

Figure 6: Transverse mass distributions for Λ, $\overline{\Lambda}$, Ξ^-, and $\overline{\Xi}^+$ hyperons in SW interactions. The WA85 Collaboration.

WA94 data are shown in table 4 where the Λ ($\overline{\Lambda}$) yields have been corrected for feed-down from Ξ ($\overline{\Xi}$) decays. The $\overline{\Lambda}/\Lambda$ and $\overline{\Xi}^+/\Xi^-$ ratios from WA85 are the same in both p-W and S-W interactions. The Ξ^-/Λ and $\overline{\Xi}^+/\overline{\Lambda}$ ratios increase, however, by about 40% when going from p-W to S-W interactions corresponding to a two and a half standard deviation effect. The WA94 results from p-S and S-S interactions are compatible with those from WA85 for p-W and S-W interactions respectively.

WA85 and WA94 have also calculated their Ξ^-/Λ and $\overline{\Xi}^+/\overline{\Lambda}$ ratios in the p_{T} interval $1 < p_{\mathrm{T}} < 2$ GeV/c in order to compare their results with those from p-p interactions. The AFS Collaboration[23] have reported a $\overline{\Xi}^+/\overline{\Lambda}$ ratio of 0.06 ± 0.02 in p-p interactions whereas WA85 and WA94 have reported values of 0.21 ± 0.03 and 0.20 ± 0.02 from S-W and S-S interactions respectively, over a factor of three larger and each corresponding to a four standard deviation difference. This difference is shown in figure 7.

The NA36 Collaboration have also measured relative hyperon and anti-hyperon production yields in S-Pb interactions employing a less central trigger than that used by WA85 and WA94. The values they report are shown

Table 4: Hyperon ratios from WA85 and WA94

Ratio	WA85 $2.3 < y_{lab} < 3.0$ $1.2 < p_T < 3.0$ GeV/c		WA94 $2.5 < y_{lab} < 3.0$ $1.2 < p_T < 3.0$ GeV/c	
	p+W	S+W	p+S	S+S
$\overline{\Lambda}/\Lambda$	0.20 ± 0.02	0.20 ± 0.01	0.22 ± 0.01	0.23 ± 0.01
$\overline{\Xi}^+/\Xi^-$	0.47 ± 0.07	0.47 ± 0.06	0.46 ± 0.05	0.55 ± 0.07
Ξ^-/Λ	0.070 ± 0.006	0.09 ± 0.006	0.078 ± 0.004	0.09 ± 0.01
$\overline{\Xi}^+/\overline{\Lambda}$	0.16 ± 0.02	0.23 ± 0.02	0.16 ± 0.02	0.21 ± 0.02

Table 5: Hyperon ratios from NA36

Ratio	NA36 S-Pb	
	Value	acceptance window
$\overline{\Lambda}/\Lambda$	0.117 ± 0.011	$2.0 < y_{lab} < 2.5$, $0.8 < p_T < 1.8$ GeV/c
$\overline{\Xi}^+/\Xi^-$	0.276 ± 0.108	$1.5 < y_{lab} < 2.5$, $0.8 < p_T < 1.8$ GeV/c
Ξ^-/Λ	0.066 ± 0.013	$2.0 < y_{lab} < 3.0$, $0.6 < p_T < 1.6$ GeV/c
$\overline{\Xi}^+/\overline{\Lambda}$	0.127 ± 0.022	$2.0 < y_{lab} < 2.5$, $0.6 < p_T < 1.6$ GeV/c

in table 5 together with the corresponding acceptance regions. The Λ and $\overline{\Lambda}$ samples have also been corrected for feed-down. It is difficult to compare NA36 results with those from WA85 and WA94 because they are for a different acceptance region. All the NA36 ratios are lower than those reported by WA85 and WA94 although the NA36 $\overline{\Xi}^+/\overline{\Lambda}$ ratio is still larger than that reported in pp interactions.

A full interpretation of these data requires a simultaneous fit to all the ratios such as that carried out by Letessier *et al.*[24]. It is also important to have the ratios in the same kinematic window.

5.1 Omega Production

WA85 was the first experiment to observe Ω^- production in heavy ion interactions. The Ω^- particles are identified through their two-step decay $\Omega^- \rightarrow K^-\Lambda(\Lambda \rightarrow p\pi^-)$. The selection procedure has been described in detail by the WA85 Collaboration[25] although it is worthwhile summarising the major procedures involved in finding this rare signal. The intersection of a

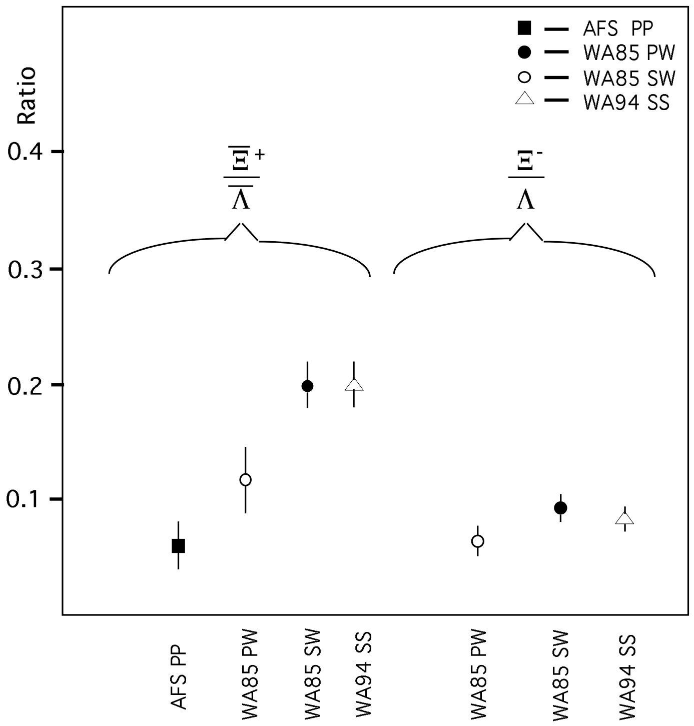

Figure 7: Ξ^-/Λ and $\overline{\Xi}^+/\overline{\Lambda}$ ratios for different interactions

Λ ($\overline{\Lambda}$) line of flight with a negative (positive) track is considered as an Ω^- candidate if the distance of closest approach is less than 2cm. Since the Ω^- signal is rare all known sources of background have to be carefully eliminated. In WA85, the main sources of a spurious Ω^- signal are:

• uncorrelated Λ and negative track combinations, mainly coming from the target,
• secondary interactions in air, and
• the reflection from the Ξ^- mass peak.

The line of flight of a Λ and a negative track will generally cross twice in the bend plane of the magnetic field. By requiring both crossings to lie inside the fiducial region, defined by the region between 100cm and 230cm downstream of the target, Λ and negative track combinations coming from the target are removed. Background from interactions in air is removed by requiring that q_{T}, the transverse momentum of the Λ decay particles with respect to the Λ line of flight, is greater than 80 MeV/c[25]. Finally, unambiguous Ω^- hyperons are selected by requiring $\cos(\theta^*) < 0.33$ where θ^* is the angle between the line of flight of the Λ and the Ω^- in the CM system, under the hypothesis that the negative track is a kaon.

The resulting (Λ K$^-$ + $\overline{\Lambda}$ K$^+$) mass spectrum is shown in figure 8. The

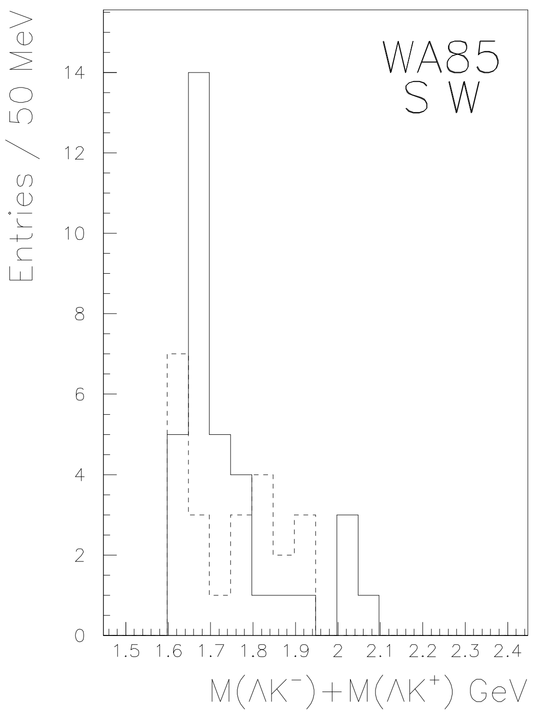

Figure 8: (Λ K$^-$ + $\overline{\Lambda}$ K$^+$) mass spectrum with the combinatorial background shown as a dashed line.

residual combinatorial background has been calculated by merging every Λ from our sample with non-Λ tracks of the previous event. Every Λ was taken once giving a sample which was automatically normalised to the full statistics. The background to the (Λ K$^-$ + $\overline{\Lambda}$ K$^+$) spectrum with the final cuts is also shown in figure 5 (dashed line). After a mass cut of ($M_\Omega - 25$) MeV < M(Λ K$^-$) < ($M_\Omega + 25$) MeV and background subtraction there are 7.0 ± 3.6 Ω^-s and 4.0 ± 2.0 $\overline{\Omega}^+$s , giving the ratio $\overline{\Omega}^+/\Omega^- = 0.57 \pm 0.41$ in the y-p_{T} region $2.5 < y_{\mathrm{lab}} < 3.0$ and $p_{\mathrm{T}} > 1.6$ GeV/c. Geometrical effects are negligible since the apparatus is left-right symmetric in the bend plane and there are approximately equal statistics with opposite magnetic field polarities.

After corrections for reconstruction efficiencies and geometrical acceptances the production ratio $(\Omega^- + \overline{\Omega}^+)/(\Xi^- + \overline{\Xi}^+) = 0.8 \pm 0.4$ in the region where good acceptance for Ω^-s and Ξ^-s overlap, $2.5 < \mathrm{y_{lab}} < 3.0$ and $p_{\mathrm{T}} > 1.6$ GeV/c. Assuming a Poisson distribution Ω^- and $\overline{\Omega}^+$ production, a 95% confidence level lower limit can be calculated yielding $(\Omega^- + \overline{\Omega}^+)/(\Xi^- + \overline{\Xi}^+) > 0.39$ [26]. The ratio has also been calculated for a given m_{T} region of $m_{\mathrm{T}} > 2.3$ GeV/c giving a ratio of $= 1.7 \pm 0.9$ (> 0.79 at 95% confidence level).

The AFS collaboration[23] have calculated a 90% upper limit on the ratio $\overline{\Omega}^+/\overline{\Xi}^+$ of 0.15 in central rapidity and $p_{\mathrm{T}} > 1.4$ GeV/c which is somewhat lower than the lower limit calculated by WA85. These comparisons are shown in figure 9.

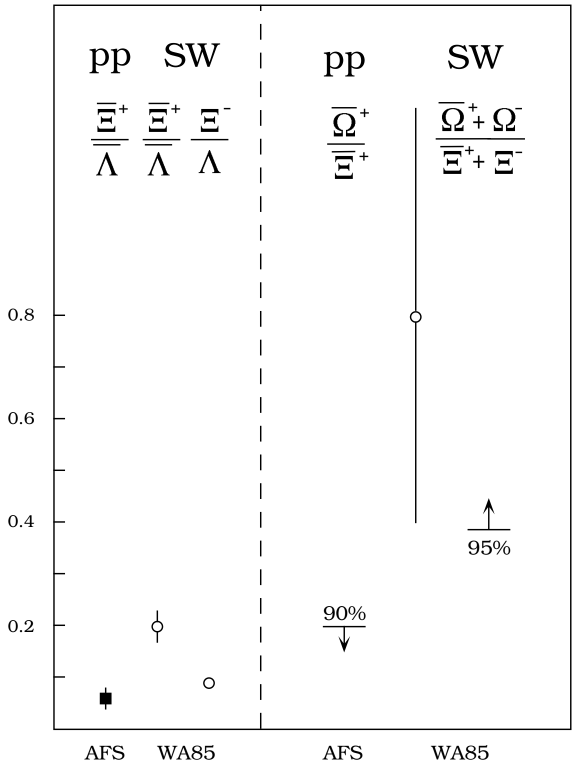

Figure 9: Comparison of Ξ^-/Λ and $(\Omega^- + \overline{\Omega}^+)/(\Xi^- + \overline{\Xi}^+)$ ratios in p-p and central S-W interactions.

6 Summary of Results from the Sulphur Beam

The data from the sulphur beams at CERN have produced a host of results on strangeness production. It has been clearly demonstrated that strange particle production is enhanced in sulphur induced interactions with respect to proton induced interactions.

Quality results are now available on transverse mass distributions for ϕ, K^+, K^-, K^0, Λ, $\overline{\Lambda}$, Ξ^-, and $\overline{\Xi}^+$ particles yielding inverse slopes of up to 240 MeV. Multiplicity and E_T distributions have shown that strangeness enhancement initially increases with the centrality of the interaction before flattening for very central events. Hyperons are enhanced by about a factor of two while the multistrange Ξ^- and $\overline{\Xi}^+$ are enhanced by a factor of about three. Ω^- and $\overline{\Omega}^+$ cascades have also been reconstructed in sulphur induced interactions which may indicate that they are enhanced even more than the other hyperons.

7 First Results from Lead-Lead Interactions

Results on strangeness production have been presented by NA44[27], NA49[28], and WA97[29]. The NA44 experiment uses a focusing spectrometer which consists of dipole and quadrupole magnets. Two highly segmented scintillator hodoscopes, a pad chamber, and two strip chambers are used for tracking and time of flight measurements. Two Čerekov detectors are used to aid particle identification.

The NA49 experiment consists of two Vertex Time Projection Chambers (VTPCs) placed into a magnetic field with two other TPCs (MTPCs) placed downstream of the VTPCs in a field-free region. A Time Of Flight system (TOF) is situated downstream of each of the two MTPCs.

The WA97 experiment employs a silicon telescope consisting of silicon pixel, microstrip, and silicon pad planes placed inside the CERN OMEGA magnet. Three multiwire pad chambers are also used as a leverarm.

Figure 10 shows preliminary mass spectra from NA49 for Λ and $\overline{\Lambda}$ hyperons and K^0s produced in Pb-Pb interactions. As can be seen from figure 10, strange particles can be cleanly reconstructed with little background in the difficult environment of Pb-Pb interactions.

7.1 Transverse Mass Spectra

WA97 have presented m_T spectra for Λ and $\overline{\Lambda}$ hyperons in p-Pb interactions which have been corrected for acceptance but not for reconstruction efficiencies or feed-down. Table 6 shows how these results compare with the

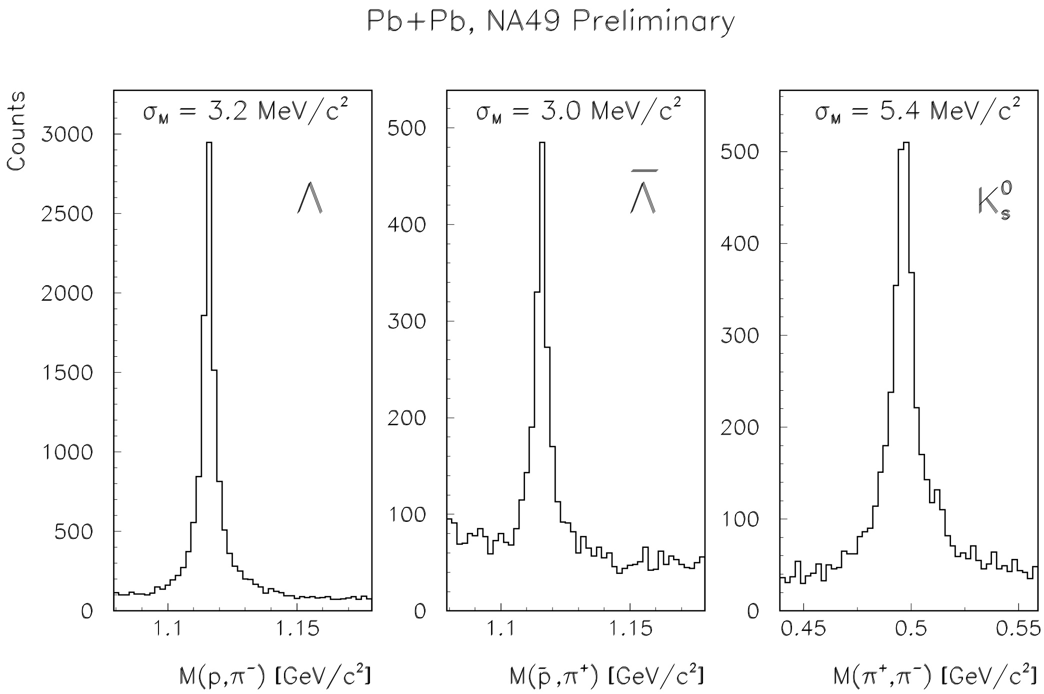

Figure 10: Effective mass spectra from NA49 of Λ, $\overline{\Lambda}$, and K^0 candidates in Pb-Pb interactions.

corresponding inverse slopes from WA85 in p-W interactions in the m_{T} range $m_{\mathrm{T}} > 1.5$ GeV.

Table 6: Inverse slopes in MeV for p-Pb and p-W interactions.

Particle	WA97 p-Pb	WA85 p-W
Λ	212 ± 7	197 ± 2
$\overline{\Lambda}$	179 ± 10	185 ± 5

As expected, they are consistent.

NA44 and NA49 have presented preliminary results on inverse slopes from Pb-Pb interactions. These results are summarised in table 7.

Table 7: Inverse slopes in MeV for Pb-Pb interactions from NA44 and NA49.

Particle	NA44 Pb-Pb	NA49 Pb-Pb
π^+	156 ± 3	188 ± 6
π^-	156 ± 15	192 ± 3
K^+	234 ± 6	224 ± 12
K^-	237 ± 9	213 ± 6
K^0		223 ± 13
p	289 ± 7	301 ± 18
$\overline{p}$	278 ± 9	291 ± 24
Λ		293 ± 10
$\overline{\Lambda}$		288 ± 10

Figure 11 shows the Λ and $\overline{\Lambda}$ transverse mass spectra from NA49 in Pb-Pb interactions in the window $2.6 < \mathrm{y_{lab}} < 3.8$, $1.0 < p_T < 2.4$ GeV/c. One

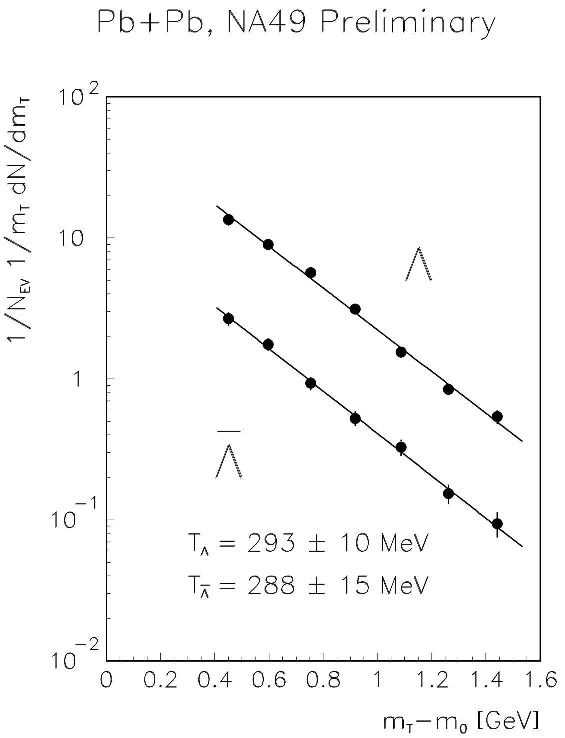

Figure 11: m_T spectra of Λ and $\overline{\Lambda}$ hyperons from NA49 in Pb-Pb interactions.

should exercise care when comparing results from different experiments due to the different acceptance regions used. It is still interesting, however, to compare table 7 with tables 2 and 3. This shows that the inverse slopes of the light mesons in Pb-Pb interactions are compatible with those in S-A interactions. The heavier baryons, however, have much larger inverse slopes in Pb-Pb interactions. This could indicate that higher temperatures are reached in the fireball resulting from a central Pb-Pb interaction or that there is more transverse flow. In practice, there is probably an increase in both.

7.2 Particle Ratios

Both NA49 and WA97 have presented preliminary $\overline{\Lambda}/\Lambda$ ratios NA49 find a $\overline{\Lambda}/\Lambda$ ratio of 0.19 ± 0.01 in the window $2.6 < \mathrm{y_{lab}} < 3.8$, $1 < p_\mathrm{T} < 2.4$ GeV/c which is compatible to that observed in S-A interactions. WA97 have presented preliminary $\overline{\Lambda}/\Lambda$ ratios for both p-Pb and Pb-Pb interactions in three p_T intervals. These are shown in table 8.

Table 8: $\overline{\Lambda}/\Lambda$ from WA97 for p-Pb and Pb-Pb interactions.

	WA97 $\overline{\Lambda}/\Lambda$ ratio	
p_T in GeV/c	p-Pb	Pb-Pb
0.6-0.9	0.27 ± 0.03	0.14 ± 0.02
0.9-1.2	0.26 ± 0.03	0.13 ± 0.02
1.2-2.0	0.23 ± 0.03	0.13 ± 0.02

As can be seen from table 8, WA97 find a lower $\overline{\Lambda}/\Lambda$ ratio in Pb-Pb than in p-Pb interactions. This is different to what was seen in sulphur induced reactions where WA85 and WA94 find the same $\overline{\Lambda}/\Lambda$ ratio in both p-A and S-A interactions. It can also been seen that the $\overline{\Lambda}/\Lambda$ ratio in Pb-Pb interactions reported by WA97 is somewhat smaller than that reported by NA49. One should note, however, that these ratios are for different rapidity intervals and there is no reason to suppose that this ratio is constant over the rapidity range $2.6 < \mathrm{y_{lab}} < 3.8$. Indeed, this ratio has been seen to vary with rapidity in SS interactions[14]. Another point to note is that neither result has been corrected for feed-down which could have a large effect depending on the selection procedures employed.

7.3 Strangeness Enhancement

NA49 have compared the average number of negative particles (h^-), K^0s, and Λs produced per event in Pb-Pb interactions with those reported from NA35 in S-S interactions. Their findings are summarised below.

- $< h^- >_{\rm PbPb} \approx 7.0 \pm 0.4 < h^- >_{\rm SS}$
- $< K^0 >_{\rm PbPb} \approx 6.5 \pm 1.3 < K^0 >_{\rm SS}$
- $< \Lambda >_{\rm PbPb} \approx 10.5 \pm 3.7 < \Lambda >_{\rm SS}$

As can be seen from above, the increase in strange particle production from S-S to Pb-Pb interactions is compatible to that of negative particles. This would suggest that although K^0s are enhanced when going from p-A to central S-A interactions they are not enhanced further when going to Pb-Pb interactions. The error on the average number of Λs per events is too large, as this stage, to determine if Λ production is enhanced or not.

7.4 Multistrange Hyperons

The WA97 Collaboration have successfully reconstructed Ξ^- and Ω^- hyperons in both p-Pb and Pb-Pb interactions. Figure 12 shows the $(\Xi^- + \overline{\Xi}^+)$ and $(\Omega^- + \overline{\Omega}^+)$ raw effective mass peaks from p-Pb and samples of their Pb-Pb data taken in 1994 and 1995.

With the current preliminary stage of the analysis, the relative normalisation between the p-Pb and Pb-Pb samples has not yet been determined. One can compare the observed $(\Omega^- + \overline{\Omega}^+)/(\Xi^- + \overline{\Xi}^+)$ ratio from p-Pb and Pb-Pb interactions, however, if one makes certain assumptions. The geometric acceptances should cancel to the first order as similar set-ups were used in the p-Pb and Pb-Pb runs. The reconstruction efficiencies should also be similar for Ξ^- and Ω^- hyperons in a given run as both particles are identified by the reconstruction of their three decay tracks. Taking the above assumptions to be correct then one would expect the Ω^- signal in the p-Pb data to be about five times stronger than that actually shown in figure 12. This would suggest, therefore, that the $(\Omega^- + \overline{\Omega}^+)/(\Xi^- + \overline{\Xi}^+)$ ratio in Pb-Pb interactions is about five times that observed in p-Pb interactions. Of course, one should remember the assumptions made above and, with the current statistics, the Ω^- enhancement is only about a two and a half standard deviation effect.

8 Summary and Conclusions

In conclusion, results from sulphur induced reactions yield a considerable strangeness enhancement with respect to proton induced reactions. Hadronic cascade models failed to reproduce the measured yields[30] and extra mechanisms such as colour ropes[31] and multiquark clusters[32] had to be introduced to describe the data. Thermodynamical QGP models describe the data well[24]. Thermodynamical models which do not invoke a QGP but

WA97 Ξ^- and Ω^- signals in p–Pb and Pb–Pb collisions

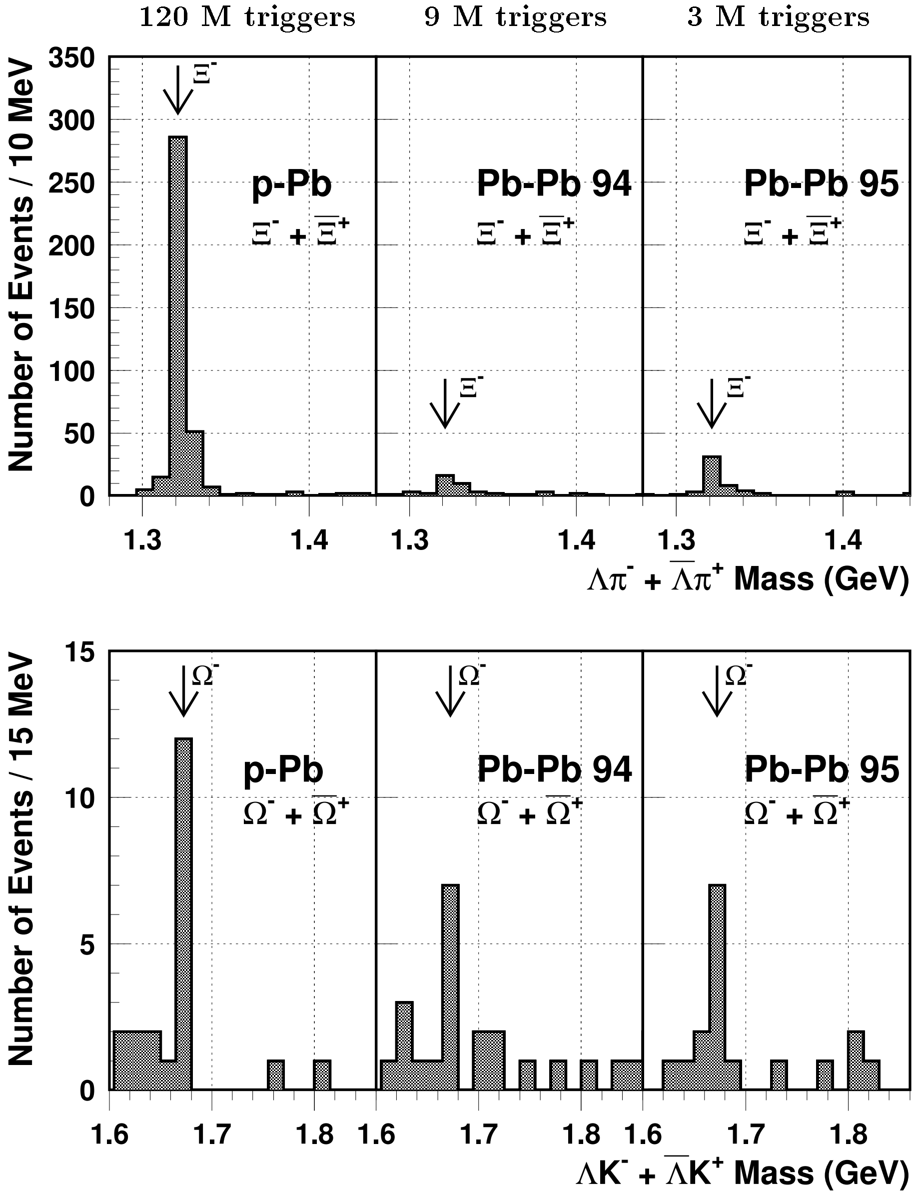

Figure 12: Uncorrected Ξ^- and Ω^- mass spectra from WA97

do assume hadrochemical equilibrium also work well but it is difficult to explain how such a short-lived system could reach equilibrium without QGP formation[2]. Whether a QGP has been created or not, the results from sulphur induced reactions do seem to suggest that a new phenomenon is apparent[30].

The first results from the lead data have shown that the new experiments work very well. The inverse slopes indicate that higher temperatures are reached and/or more transverse flow occurs in Pb-Pb collisions. It is not yet clear, with the current statistics, whether Λs are enhanced further in Pb-Pb interactions with respect to S-A reactions. There are, however, indications that Ω^- production could be greatly enhanced with respect to proton induced reactions. There will soon be much higher statistics available and the results could be very exciting indeed.

Acknowledgements

I should like to thank J.B. Kinson and O. Villalobos Baillie for their useful comments and suggestions while preparing this review. I should also like to thank R. Lietava for his generous hospitality during my visit to Bratislava.

References

[1] J. Rafelski and R. Hagedorn, in *Statistical Mechanics of Quarks and Hadrons*, ed. H. Satz (North Holland, Amsterdam, 1981).
J. Rafelski and B. Müller, Phys. Rev. Lett. **48** (1982) 1066

[2] U. Heinz, Nucl. Phys. **A566** (1994) 205c

[3] T. Matsui, B. Svettisky and L.D. McLerran, Phys. Rev. **D34** (1986) 2047.
K.S. Lee, M. Rhoades-Browne and U. Heinz, Phys. Rev. **C31** (1988) 1452.

[4] H. C. Eggers and J. Rafelski, Int. J. Mod. Phys. **A6** (1991) 1067.

[5] J.-P. Guillaud, Nucl. Phys. **A525** (1991) 449c.
A. Baldisseri, Nucl. Phys. B (Proc. Suppl.) **16** (1990) 397.

[6] M.C. Abreu *et al.* Nucl. Phys. **A566** (1994) 77c.

[7] M.A. Mazzoni, Nucl. Phys. **A566** (1994) 95c.

[8] M. Masera, Nucl. Phys. **A590** (1995) 93c.

[9] P. Koch, U. Heinz, and J. Pišút, phys. Lett. **B243** (1990) 149.

[10] The NA35 Collab., J. Bartke *et al.*, Z. Phys. **C48** (1990) 191.

[11] The WA85 Collab., D. Evans *et al.*, Nucl. Phys. **A566** (1994) 225c.

[12] The WA85 Collab., S. Abatzis *et al.*, Phys. Lett. **B244** (1990) 130.
The WA85 Collab., D. Evans *et al.*, Proc. Hadron Structure 92, Stará Lesná, Czechoslovakia, (1992) 257.

[13] The NA36 Collab., E. Andersen *et al.*, Phys. Lett. **B316** (1993) 603.
The NA36 Collab., J.M. Nelson *et al.*, Nucl. Phys. **A566** (1994) 217c.

[14] The NA35 Collab., T. Alber *et al.*, Z. Phys. **C64** (1994) 195.

[15] The NA35 Collab., J. Baechler *et al.*, Z. Phys. **C58** (1993) 367.

[16] The NA36 Collab., E. Andersen *et al.*, Phys. Lett. **B294** (1992) 127.

[17] The WA85 Collab., S. Abatzis *et al.*, Phys. Lett. **B359** (1995) 382.
J. Paul Davies, Ph.D. Thesis, The University of Birmingham, January 1996, RAL-TH-96-002.
The WA85 Collab., D. Evans *et al.*, Strangeness '96, Budapest, Hungary, May 1996, to be published in APH N.S., Heavy Ion Physics.

[18] The WA85 Collab., S. Abatzis *et al.*, Phys. Lett. **B355** (1995) 401.
The WA85 Collab., D. Di Bari *et al.*, Nucl. Phys. **A590** (1995) 307c.

[19] The WA85 Collab., S. Abatzis *et al.*, Phys. Lett. **B376** (1996) 251.

[20] The WA94 Collab., S. Abatzis *et al.*, Phys. Lett. **B354** (1995) 178.
The WA94 Collab., M. Venables *et al.*, Strangeness '96, Budapest, Hungary, May 1996, to be published in APH N.S., Heavy Ion Physics.

[21] The WA94 Collab., J.B. Kinson *et al.*, Nucl. Phys. A590 (1995) 317c.

[22] The NA36 Collab., E. Andersen *et al.*, Phys. Lett. **B327** (1994) 433.

[23] AFS Collab., T. Åkesson et al., Nucl. Phys. **B246** (1984) 1-11.

[24] J. Letessier, A. Tounsi, U. Heinz, J. Sollfrank, and J. Rafelski, Phys. Rev. Lett. **70** (1993) 3530.
J. Letessier, A. Tounsi, U. Heinz, J. Sollfrank, and J. Rafelski, Phys. Rev. **D51** (1995) 3408.

[25] The WA85 Collab., S. Abatzis *et al.*, Phys. Lett. **B316** (1993) 615.

[26] The WA85 Collab., S. Abatzis *et al.*, Phys. Lett. **B347** (1995) 158.

[27] The NA44 Collab., Nu Xu *et al.*, Quark Matter '96, Heidelberg, Germany, May 1996, to be published in Nucl. Phys. **A**.

[28] The NA49 Collab., P.G. Jones *et al.*, Quark Matter '96, Heidelberg, Germany, May 1996, to be published in Nucl. Phys. **A**.

[29] The WA97 Collab., H. Helstrup *et al.*, Quark Matter '96, Heidelberg, Germany, May 1996, to be published in Nucl. Phys. **A**.

[30] B. Müller, Nucl. Phys. **A590** (1995) 3c.

[31] H. Sorge, M. Berenguer, H. Stöcker, and W. Greiner, Phys. Lett. **B289** (1996) 6.

[32] J. Aichelin and K. Werner, Phys. Lett. **B300** (1993) 158.